Talanta 96 (2012) 168–173

Contents lists available at SciVerse ScienceDirect

Talanta

journal homepage: www.elsevier.com/locate/talanta

A dual-electrode flow sensor fabricated using track-etched microporous membranes☆

Hitoshi Mizuguchi[a,*], Kanako Shibuya[a], Azumi Fuse[a], Tomoko Hamada[a], Masamitsu Iiyama[b], Kazuhiro Tachibana[a], Tatsuo Nishina[a], Junichi Shida[a]

[a] Graduate School of Science and Engineering, Yamagata University, Yonezawa, 992-8510, Japan
[b] Nomura Micro Science Co. Ltd., 2-4-37, Okada, Atsugi-shi, Kanagawa, 243-0021, Japan

ARTICLE INFO

Article history:
Available online 27 February 2012

Keywords:
Dual-electrode system
Electrochemical flow cell
Flow injection analysis
Collection efficiency
Track-etched membrane filter

ABSTRACT

A new dual-electrode flow sensor has been fabricated by piling the microporous membrane electrodes which have 7–10 μm thickness. The electrode was prepared by sputtering of platinum onto both sides of the membrane filter which contain a smooth flat surface as well as cylindrical pores with uniform diameters. The electrolysis is performed when the sample solution flows through the membrane electrode, and a generated analyte on the first working electrode is instantaneously transported to the surface of second working electrode which is located at the downstream of the first one. In this case, the sample solution surely flows through the pores of the membrane filters. As the result, highly efficient electrolysis was achieved at each electrode, and the collection efficiency values as high as 100% were obtained in the wide range of flow rate. Good responses to the injections of sample solutions were also confirmed in the FIA system.

1. Introduction

Dual-electrode system consists of two working electrodes which are arranged in the direction of flow of sample solution [1]. The potentials of these electrodes are controlled individually, and the products by electrolysis at the first electrode (the generator electrode) are carried to the second electrode (the collector electrode) by hydrodynamic flow. In this case, collection efficiency is defined as the ratio of the collector current to the generator current. This value is the percentage of the material generated at the first electrode which is detected at the second electrode, and is an important parameter for dual-electrode system. In this analytical mode, monitoring the current of each electrode provides valuable information on the reaction at the electrode surface. These methods have been largely used for investigating reaction mechanisms and related redox chemistry in various areas such as fuel cell, rechargeable battery, plating, corrosion, biomaterials, *etc.*

Rotating ring-disk electrode (RRDE) [2] is one of the most frequently used dual-electrode system. RRDE consists of a disk and ring electrode material embedded in a rod of an insulating material. The product formed at the disk electrode is swept over to the ring electrode by convectively radial flow caused by rotation of the electrode. On the other hand, channel flow double electrode (CFDE) [3] has also been used as a superior dual-electrode system. CFDE is based on a thin layer of solution flowing parallel to two planar electrode surfaces embedded in a rectangular channel. These techniques have been described theoretically by many researchers [4–10]. Other dual-electrode systems available in electrochemistry include the wall-jet ring-disk electrode [11–14], the double tubular electrode [15], a twin-electrode thin-layer cell [16,17], and a dual thin-layer flow cell with a double-disk electrode [18]. Dual-electrode systems with microelectrodes, such as a dual microband electrode [19,20], a dual micro-disk electrode [21,22], a twin interdigitated electrode [23–27], a micro-disk array [28], microarrays of ring-recessed disk electrodes [29–31], a ring-disk ultramicroelectrode [32–34], and a paired gold electrode junction [35–37], *etc.*, have also been widely utilized in voltammetric analysis since the 1980s.

In flow analysis area, numerous reports have described various analytical techniques with dual-electrode system [38–50] to eliminate interfering species prior to analytical steps [44–47], to generate titrating species for indirect detections [48], or to obtain signal amplification by means of redox cycling [44,46,49,50]. Some dual-electrode system with high collection efficiency has been developed by decreasing the solution layer thickness [14,42,51]. In the case of the thin-layered channel flow electrode or wall-jet ring-disk electrode, it is expected that the collection efficiency will

☆ The part of this work was presented at the 51st chemical sensor symposium in an annual meeting of the Electrochemical Society of Japan, whose abstract paper was published in *Chemical Sensors*, 2011, vol. 27 Supplement A, pp. 67–69.

* Corresponding author.
E-mail address: mizu@yz.yamagata-u.ac.jp (H. Mizuguchi).

0039-9140/$ – see front matter © 2012 Elsevier B.V. All rights reserved.
doi:10.1016/j.talanta.2012.02.001

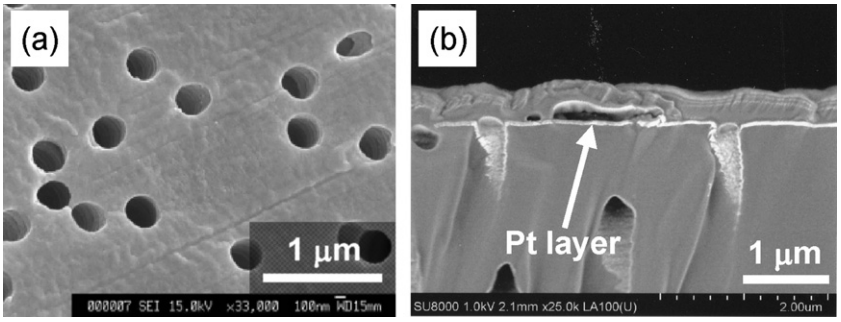

Fig. 1. SEM images of microporous membrane electrode. (a) Surface of the electrode. (b) Cross sectional view after the treatment by ion milling. Pore size of the electrode was 0.4 μm.

increase up to nearly 100% by decreasing the thickness of solution layer, when the electrode size is large and the flow rate is sufficiently low. However, it takes a long time to reach a detector at low flow rate. Making the flow rate or the distance between the electrodes too much small causes another problems such as the diffusion of the material generated at the first electrode against the direction of flow [48,51].

This study is intended to develop a high-performance dual-electrode system, that is, keeping high collection efficiency in wide range of the flow rate. Kenkel and Bard [52] described a dual electrode coulometric flow cell with porous silver electrodes, and the collection efficiency of electrogenerated material approached 100%. In this study, the microporous membrane electrodes were prepared by sputtering of platinum on both the surfaces of a track-etched membrane filter, which has 7–10 μm thickness. The membrane filters made of polycarbonate contain a smooth flat surface as well as cylindrical pores with uniform diameters. In this case, the sample solution surely flows through the pores of the membrane filters. It has been found that the microporous membrane electrode prepared here enables efficient electrolysis in a flow condition while the sample solution flows through the electrode. Furthermore, a dual-electrode has been fabricated merely by piling the platinum sputtered membrane filter. Because of the highly efficient electrolysis at each electrode, collection efficiency values as high as 100% were obtained in voltammetric experiments performed with potassium ferricyanide. In the discussion below, a superior performance of the new dual-electrode system with microporous membrane electrodes is demonstrated by using an electrochemical flow cell which is constructed for this proposed dual-electrode system.

2. Experimental

2.1. Preparation of the microporous membrane electrode

The membrane filters employed as template of the microporous membrane electrode were Nuclepore™ track-etched membrane filter (Whatman). Martin and co-workers [53] described the preparation of ensembles of microscopic electrodes using this membrane filter as a template. The electrodes which were used in this study were fabricated by coating platinum onto both sides of the membrane filter using an auto fine coater (Model JFC-1600; JEOL Ltd., Japan). The substrate–target distance, current, and sputtering time were set to 52 mm, 40 mA, and 300 s, respectively. The SEM images of the microporous membrane electrode are shown in Fig. 1. It is confirmed that the smooth flat surface of the filter and entrance of the pores are modified with platinum. The thickness of platinum layer is approximately 100 nm. These electrodes were set in the flow cell as described below, and were treated electrochemically by 50 times cycling of a linear sweep potential between 0 and 0.8 V *vs.* Ag/AgCl (100 mV s^{-1}) in 0.5 M potassium chloride solution, prior to recording all experimental data. The electrodes used in this study were freshly prepared for each series of experimental runs.

2.2. Structure of the electrochemical flow cell

The structure of the electrochemical flow cell is shown in Fig. 2. The microporous membrane electrodes were sequentially arranged as the generator, collector, and counter electrode along the flow of the sample solution by alternately piling up the electrodes and unmodified membrane filters. Insertion of the unmodified membrane filter as a spacer between the generator and collector electrodes avoids short-circuits and keeps a completely uniform distance between the electrodes. The pore size of the membrane filters which was used as a spacer or a cover was 5.0 μm. The electrodes were sandwiched between two parts of the flow cell in which a hole of 2 mm in the diameter was drilled. The membrane electrodes were supported with a line filter made of PTFE (No. 6010-54000; GL Science Inc., Japan) of 4 mm in a diameter on the fundamental part of the flow cell. A screw type reference electrode (Model RE-3VP silver–silver chloride; ALS Inc.) was put at a 10 mm downstream of the counter electrode.

2.3. Apparatus and methods

The apparatus for evaluation of the dual-electrode system was shown in Fig. 3. For the measurement, the solutions were made to flow by pressurizing the solution tank using argon gas (>99.999%), and flow rates were determined by measuring the volume of solution collected in a graduated cylinder during a standard time. In the continuous flow mode, the sample solution was kept in the tank and flowed into the electrochemical flow cell continuously *via* PTFE tubing of 2 mm ID and 3 mm OD. The electrodes mounted on the flow cell were connected to a bi-potentiostat

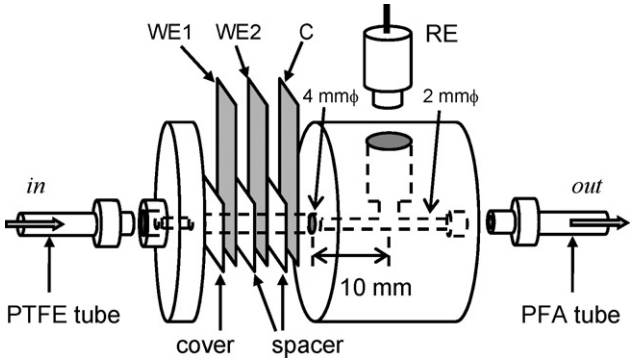

Fig. 2. Structure of the flow cell constructed in this study. WE1: generator electrode, WE2: collector electrode, CE: counter electrode, RE: reference electrode.

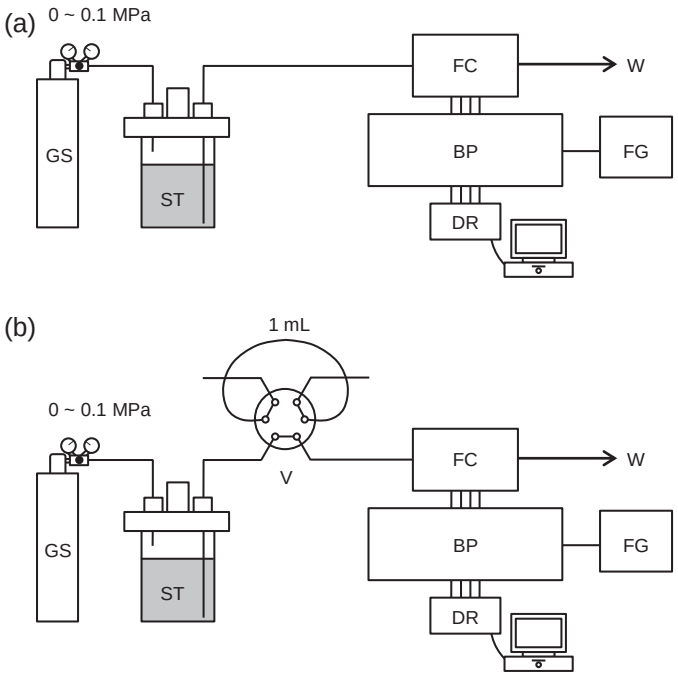

Fig. 3. Apparatus for evaluation of device performance. (a) Continuous flow mode. (b) Sample injection mode. GS: argon gas cylinder, ST: solution tank, FC: flow cell, BP: bi-potentiostat, DR: data recorder, FG: function generator, V: 6-port injection valve.

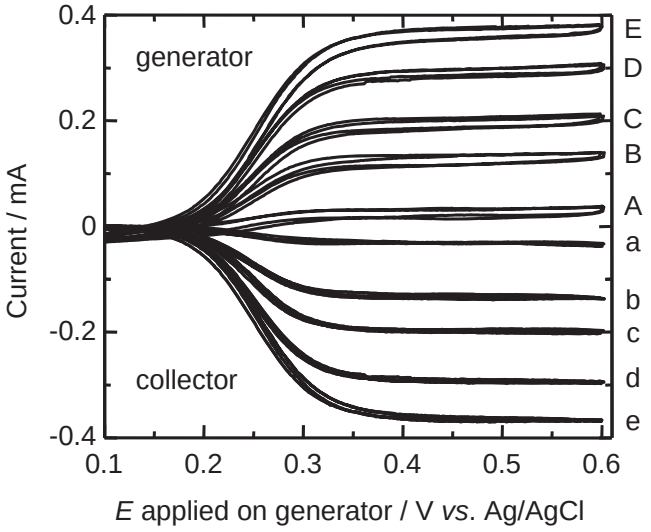

Fig. 4. Hydrodynamic voltammograms recorded at generator (A–E) and collector (a–e) electrodes. The pore size of the membrane filter used as a template of the electrodes was 0.4 μm. Sample solution was 0.30 mM $Fe(CN)_6^{4-}$ with 0.5 M KCl. The potential of the generator electrode was swept between 0.1 and 0.6 V *vs.* Ag/AgCl with a scan rate of 20 mV s^{-1}. The potential of the collector electrode was held at 0.1 V *vs.* Ag/AgCl. Flow rate values of the sample solution were 0.09 (A, a), 0.27 (B, b), 0.43 (C, c), 0.56 (D, d), and 0.78 ml min^{-1} (E, e).

(Model HA1010mM2B; Hokuto Denko Co., Japan) equipped with a function generator (Model HB-111A; Hokuto Denko Co.) and a data recorder (Model GL200A; GRAPHTEC Co., Japan). In the sample injection mode, a 6-port valve was connected between a solution tank and the flow cell. The sample solutions were injected to the carrier electrolyte (0.5 M KCl). Potassium hexacyanoferrate(II) solution was used as a sample solution throughout this work. This sample solution was prepared by dissolving potassium hexacyanoferrate(II) trihydrate (Kanto Chemical Co., Inc.) in deionized water and adding appropriate amount of 3 M potassium chloride solution. Argon gas (>99.999%) was passed through the sample solution for 20 min prior to electrochemical measurements. All the experiments were conducted under room temperature (25 ± 1 °C). All reported currents have corrected by subtracting the background current observed at the same flow rate for solutions not containing the electroactive species. The electrochemical active surface area of the electrode was determined from integration of the charge of oxidation of the adsorbed hydrogen region of the stationary cyclic voltammetry after subtracting the double layer charge and use 210 μC/real cm^2 as the saturation coverage.

3. Results and discussion

3.1. Hydrodynamic voltammogram and limiting currents

The typical hydrodynamic voltammograms recorded at the generator and the collector electrodes are shown in Figs. 4 and 5. In this experiment, the potential of the generator electrode was swept between 0.1 and 0.6 V *vs.* Ag/AgCl with a scan rate of 20 mV s^{-1}, and the potential of the collector electrode was held at 0.1 V *vs.* Ag/AgCl. The characteristic sigmoidal responses were observed in both voltammograms. An increase in limiting current at generator and collector electrode was noticed as the flow rate increase, and was greatly dependent on a pore size. Dependence of the redox currents on the flow rate was shown in Fig. 6. In this experiment, the potentials of the generator and collector electrodes were held at 0.5 and 0.1 V *vs.* Ag/AgCl, respectively. The dashed lines represent calculated values for 100% efficiency of oxidation and reduction. It can be seen that the limiting currents approach the dashed lines as the pore size and the flow rate become small. When the pore size of the membrane filter used was 0.4 μm, the redox currents on both generator and collector electrodes were found to be proportional to the flow rate. In this study, the freshly prepared electrodes were used for each series of experimental runs. Except the case

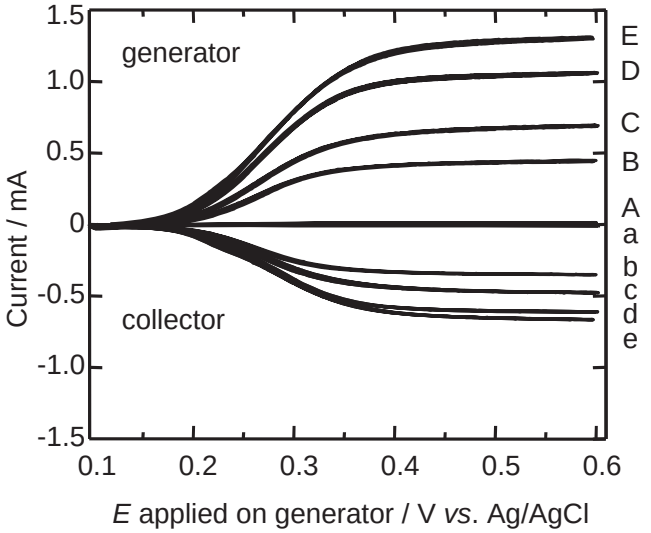

Fig. 5. Hydrodynamic voltammograms recorded at generator (A–E) and collector (a–e) electrodes. The pore size of the membrane filter used as a template of the electrodes was 5.0 μm. Sample solution was 1.0 mM $Fe(CN)_6^{4-}$ with 0.5 M KCl. The potential of the generator electrode was swept between 0.1 and 0.6 V *vs.* Ag/AgCl with a scan rate of 20 mV s^{-1}. The potential of the collector electrode was held at 0.1 V *vs.* Ag/AgCl. Flow rate values of the sample solution were 0.14 (A, a), 0.38 (B, b), 0.68 (C, c), 1.3 (D, d), and 1.8 ml min^{-1} (E, e).

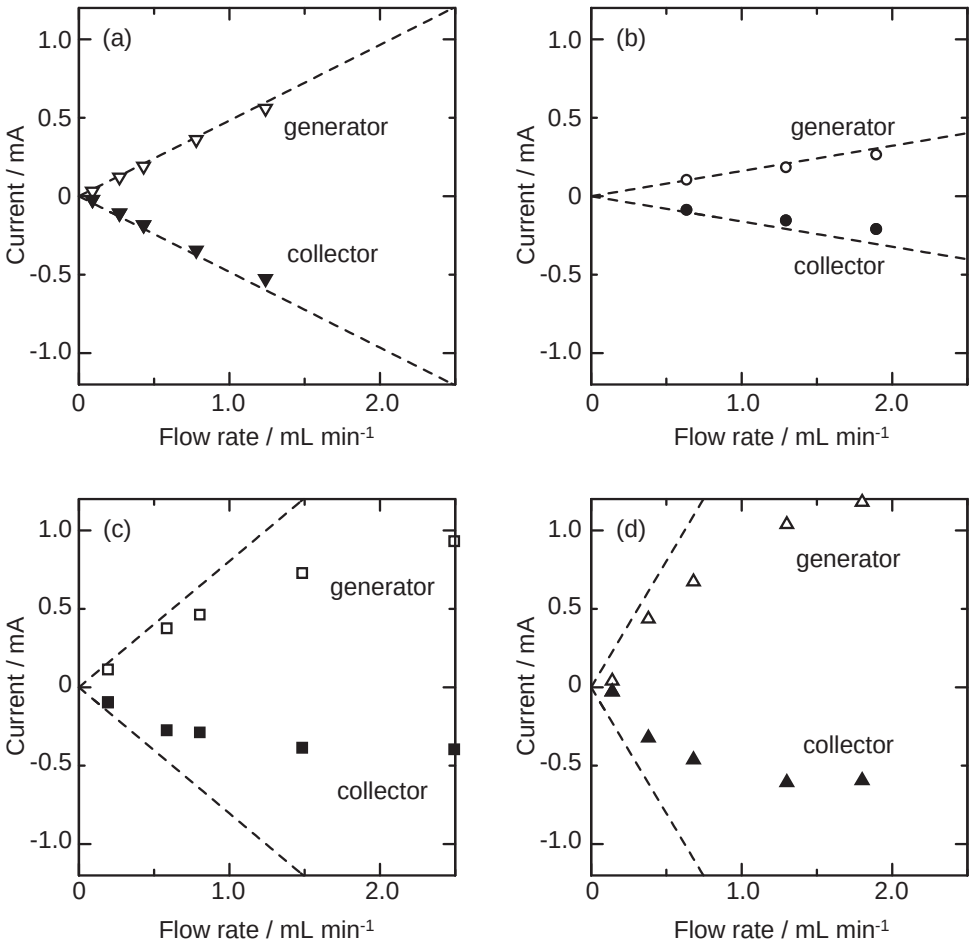

Fig. 6. Effect of flow rate on the limiting currents. The pore sizes of the membrane filter used as a template of the electrodes were 0.4 (a), 1.0 (b), 3.0 (c), and 5.0 μm (d). The concentration of $Fe(CN)_6^{4-}$ were 0.30 (a), 0.10 (b), 0.50 (c), and 1.0 mM (d). The supporting electrolyte was 0.5 M KCl. The potentials of the generator and collector electrodes were held at 0.5 and 0.1 V *vs.* Ag/AgCl, respectively.

that the sample solution was hard to be flowed through the piled electrodes because of a defective product of template filters, these data were reproduced even if another electrode freshly prepared were used.

3.2. Efficiency of electrolysis

By Faraday's law, the generator current (i_{WE1}) can be related to flow rate (v) and concentration (c) by the following equation:

$$i_{WE1} = nFcvf_c \quad (1)$$

where n, F, and f_c are the number of electron, the Faraday constant, and the conversion efficiency. The conversion efficiency which is rate of electrolysis usually depends on flow rate, electrode dimension, and conformation. For total conversion on passage through the electrode, f_c equals 1. The collection efficiency N, which is a measure of the percentage of the material generated at the first electrode which is detected at the second electrode, is expressed as follow:

$$N = \frac{i_{WE2}}{i_{WE1}} \quad (2)$$

where i_{WE1} and i_{WE2} are the generator current and the collector current, respectively. As shown in Fig. 7, the electrode of which pore size was 0.4 μm brought about the conversions greater than 96% in the flow rate up to 1.2 ml min^{-1}. On the other hand, when the pore size of the membrane filter used as a template of the electrodes was 1.0, 3.0, or 5.0 μm, the conversion efficiency were remarkably decreased with increase of the flow rate. The collection efficiency tended similar to the conversion efficiency. When the pore size of the membrane filter used as a template of the electrodes was 0.4 μm, greater than 95% of the collection efficiencies were obtained in the flow rate up to 1.2 ml min^{-1}. The electrochemical active surface areas of these electrodes whose pore sizes were 0.4, 1.0, and 5.0 μm were measured to be 4.7, 4.2, and 4.1 cm^2, respectively. Although the active surface area of these electrodes was almost the same, there was a clear difference in electrochemical reaction efficiency. These results show that the pore size greatly contributes to the reaction efficiency because of the sufficiently shorter length of diffusion of the electro-active species in flowing through the pores.

3.3. Amperometric response in flow injection analysis

The amperometric response of the electrodes was examined with the sample injection mode (Fig. 3(b)). Sample solutions were injected by using a 6-port valve equipped with a 1 ml sample loop. The potentials of the generator and collector electrodes were held at 0.5 and 0.1 V *vs.* Ag/AgCl, respectively. Fig. 8 shows the results obtained by injecting solutions containing hexacyanoferrate(II) ion in various concentrations in the FIA system. There is a very

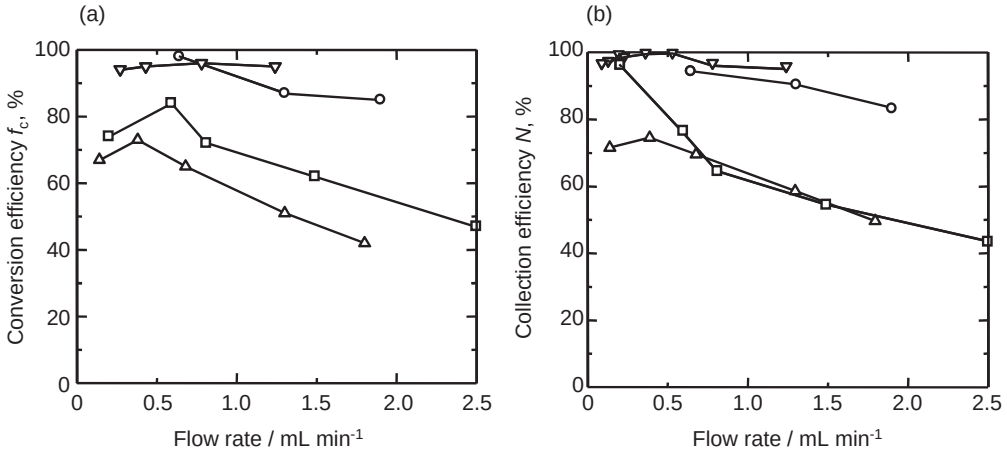

Fig. 7. Influence of the flow rate on the conversion efficiency (a) and collection efficiency (b). The potentials of the generator and collector electrodes were held at 0.5 and 0.1 V *vs.* Ag/AgCl, respectively. The pore size of the membrane filter used as a template of the electrodes was 0.4 (▽), 1.0 (○), 3.0 (□), and 5.0 μm (△).

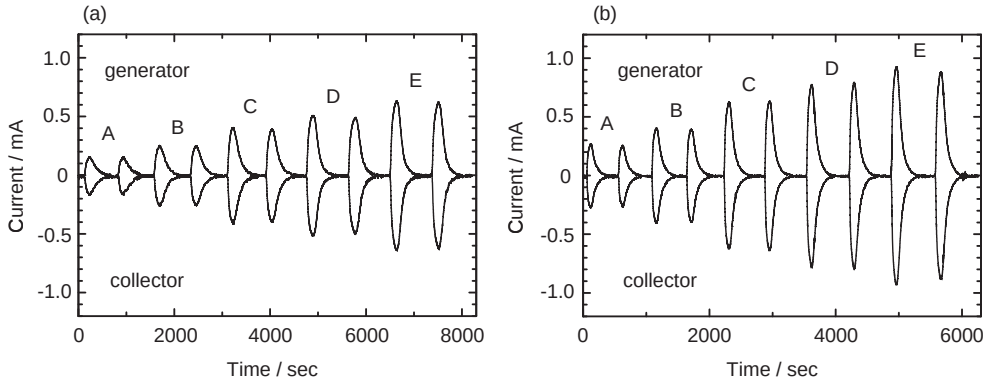

Fig. 8. Simultaneous signal recordings at the generator and collector electrode during injections of sample solutions containing $Fe(CN)_6^{4-}$ (0.30 (A), 0.50 (B), 0.80 (C), 1.0 (D), and 1.2 mM (E)) to the carrier electrolyte (0.5 M KCl). Flow rate values were 0.38 (a) and 0.60 ml min^{-1} (b). The potentials of the generator and collector electrodes were held at 0.5 and 0.1 V *vs.* Ag/AgCl, respectively. The pore size of the membrane filter used as a template of the electrodes was 0.4 μm.

small delay between the anodic and the corresponding cathodic current, and good responses were obtained. As shown in Fig. 9, it was confirmed that the maximum current, which is peak height, is proportional to concentration of the analyte.

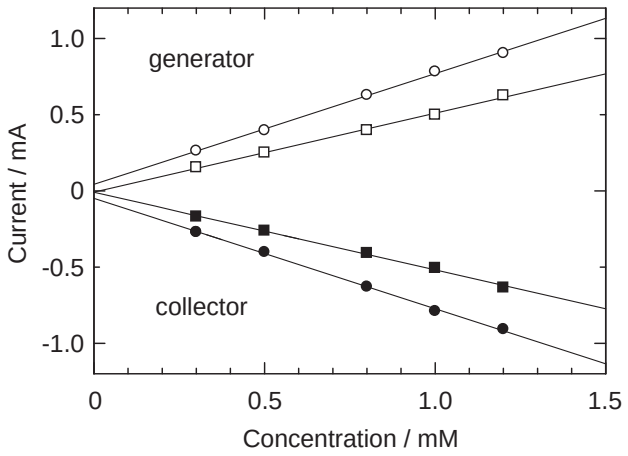

Fig. 9. Relationship between concentration $Fe(CN)_6^{4-}$ and signal peak height. Flow rate values were 0.38 (□, ■) and 0.60 ml min^{-1} (○, ●). The experimental conditions were same as Fig. 8.

4. Conclusion

In conclusion, a new dual-electrode system was fabricated using track-etched membrane filters. This system has high conversion efficiency and high collection efficiency in the wide range of flow rate. The authors emphasize the simple structure and easy fabrication as well as superior performance of this dual-electrode system. The proposed device would be useful detector in flow injection analysis.

Acknowledgments

This work was supported by Grant-in-Aid for Science Research No. 22750065 from the Ministry of Education, Culture, Sports, Science and Technology of Japan. The authors thank to Mr. Noboru Imoto (technical staff member at Yamagata University) for helpful assistance in the construction of the flow cell.

References

[1] A.J. Bard, L.R. Faulkner, Electrochemical Methods: Fundamentals and Applications, second ed., Wiley, New York, 2001.
[2] A. Frumkin, L. Nekrasov, B. Levich, Ju. Ivanov, J. Electroanal. Chem. 1 (1959) 84–90.
[3] H. Gerischer, I. Mattes, R. Braun, J. Electroanal. Chem. 10 (1965) 553–567.
[4] H. Matsuda, J. Electroanal. Chem. 16 (1968) 153–164.
[5] R. Braun, J. Electroanal. Chem. 19 (1968) 23–35.

[6] K. Tokuda, H. Matsuda, J. Electroanal. Chem. 44 (1973) 199–212.
[7] K. Tokuda, H. Matsuda, J. Electroanal. Chem. 52 (1974) 421–431.
[8] K. Aoki, K. Tokuda, H. Matsuda, J. Electroanal. Chem. 79 (1977) 49–78.
[9] K. Aoki, H. Matsuda, J. Electroanal. Chem. 94 (1978) 157–163.
[10] K. Aoki, K. Tokuda, H. Matsuda, J. Electroanal. Chem. 195 (1985) 229–249.
[11] R.G. Compton, A.C. Fisher, M.H. Latham, C.M.A. Brett, A.M.C.F. Oliveira Brett, J. Appl. Electrochem. 22 (1992) 1011–1016.
[12] W.J. Albery, C.M.A. Brett, J. Electroanal. Chem. 148 (1983) 201–210.
[13] W.J. Albery, C.M.A. Brett, J. Electroanal. Chem. 148 (1983) 211–220.
[14] K. Toda, S. Oguni, Y. Takamatsu, I. Sanemasa, J. Electroanal. Chem. 479 (1999) 57–63.
[15] M. Thompson, R.G. Compton, J. Electroanal. Chem. 583 (2005) 318–326.
[16] B. McDuffie, L.B. Anderson, C.N. Reilley, Anal. Chem. 38 (1966) 883–890.
[17] T.R.L.C. Paixão, E.M. Richter, J.G.A. Brito-Neto, M. Bertotti, J. Electroanal. Chem. 596 (2006) 101–108.
[18] Z. Jusys, J. Kaiser, R.J. Behn, Electrochim. Acta 49 (2004) 1297–1305.
[19] J.E. Bartelt, M.R. Deakin, C. Amatore, R.M. Wightman, Anal. Chem. 60 (1988) 2167–2169.
[20] H. Rajantie, J. Strutwolf, D.E. Williams, J. Electroanal. Chem. 500 (2001) 108–120.
[21] J.E. Baur, P.N. Motsegood, J. Electroanal. Chem. 572 (2004) 29–40.
[22] I.J. Cutress, Y. Wang, J.G. Limon-Petersen, S.E.C. Dale, L. Rassaei, F. Marken, R.G. Compton, J. Electroanal. Chem. 655 (2011) 147–153.
[23] D.G. Sanderson, L.B. Anderson, Anal. Chem. 57 (1985) 2388–2393.
[24] A.J. Bard, J.A. Crayston, G.P. Kittlesen, T.V. Shea, M.S. Wrighton, Anal. Chem. 58 (1986) 2321–2331.
[25] C.E. Chidsey, B.J. Feldman, C. Lundgren, R.W. Murray, Anal. Chem. 58 (1986) 601–607.
[26] K. Aoki, M. Morita, O. Niwa, H. Tabei, J. Electroanal. Chem. 256 (1988) 269–282.
[27] O. Niwa, M. Morita, H. Tabei, Anal. Chem. 62 (1990) 447–452.
[28] T. Horiuchi, O. Niwa, M. Morita, H. Tabei, J. Electroanal. Chem. 295 (1990) 25–40.
[29] D. Menshykau, F.J. del Campo, F.X. Munoz, R.G. Compton, Sens. Actuators B 138 (2009) 362–367.
[30] D. Menshykau, A.M. O'Mahony, F.J. del Campo, F.X. Munoz, R.G. Compton, Anal. Chem. 81 (2009) 9372–9382.
[31] D. Menshykau, M. Cortina-Puig, F.J. del Campo, F.X. Munoz, R.G. Compton, J. Electroanal. Chem. 648 (2010) 28–35.
[32] G. Zhao, D.M. Giolando, J.R. Kirchhoff, Anal. Chem. 67 (1995) 1491–1495.
[33] P. Liljeroth, C. Johans, C.J. Slevin, B.M. Quinn, K. Kontturi, Elecrtochem. Commun. 4 (2002) 67–71.
[34] P. Liljeroth, C. Johans, C.J. Slevin, B.M. Quinn, K. Kontturi, Anal. Chem. 74 (2002) 1972–1978.
[35] R.W. French, A.M. Collins, F. Marken, Electroanalysis 20 (2008) 2403–2409.
[36] R.W. French, F. Marken, J. Solid State Electrochem. 13 (2009) 609–617.
[37] L. Rassaei, R.W. French, R.G. Compton, F. Marken, Analyst 134 (2009) 887–892.
[38] J.C. Hoogvliet, F. Elferink, C.J. van der Poel, W.P. van Bennekom, Anal. Chim. Acta 153 (1983) 149–159.
[39] D.-T. Chin, R.R. Chandran, J. Electrochem. Soc. 128 (1981) 1904–1912.
[40] L.E. Fosdick, J.L. Anderson, T.A. Baginski, R.C. Jaeger, Anal. Chem. 58 (1986) 2750–2756.
[41] H. Ji, E. Wang, Talanta 38 (1991) 73–80.
[42] O. Niwa, M. Morita, B.P. Solomon, P.T. Kissinger, Electroanalysis 8 (1996) 427–433.
[43] J.A. Cooper, R.G. Compton, Electroanalysis 10 (1998) 141–155.
[44] A. Aoki, T. Matsue, I. Uchida, Anal. Chem. 62 (1990) 2206–2210.
[45] M. Zhao, D.B. Hibbert, J.J. Gooding, Anal. Chem. 75 (2003) 593–600.
[46] K. Hayashi, Y. Iwasaki, R. Kurita, K. Sunagawa, O. Niwa, A. Tate, J. Electroanal. Chem. 579 (2005) 215–222.
[47] X. Xu, S.G. Weber, J. Electroanal. Chem. 630 (2009) 75–80.
[48] T.R.L.C. Paixão, R.C. Matos, M. Bertotti, Electochim. Acta 48 (2003) 691–698.
[49] H. Tabei, M. Takahashi, S. Hoshino, O. Niwa, T. Horiuchi, Anal. Chem. 66 (1994) 3500–3502.
[50] O. Niwa, M. Morita, Anal. Chem. 68 (1996) 355–359.
[51] C. Amatore, N. Da Mota, C. Lemmer, C. Pebay, C. Sella, L. Thouin, Anal. Chem. 80 (2008) 9483–9490.
[52] J.V. Kenkel, A.J. Bard, J. Electroanal. Chem. 54 (1974) 47–54.
[53] M. Wirtz, S. Yu, C.R. Martin, Analyst 127 (2002) 871–879.